Spin-contamination of coupled-cluster wave functions

Anna I. Krylov
Department of Chemistry, University of Southern California, Los Angeles, California 90089

(Received 16 June 2000; accepted 21 July 2000)

The propensity of approximate solutions of the electronic Schrödinger equation to break spin-symmetry is directly related to the quality of the approximate wave function, and thus can be used as a diagnostic tool. The quasi-variational nature of the (valence) optimized orbitals coupled-cluster doubles methods, (V)OO-CCD, enables a discussion of the stability of coupled-cluster wave functions in terms of both spin-contamination and a corresponding energy lowering relative to the pure spin solutions. The spin-contamination of (V)OO-CCD models has been studied for bond-breaking processes and diradicals. The main findings are: (i) The OO-CCD method is stable for a relatively large range of nuclear distortions and is capable of eliminating even very large spin-contamination of the unrestricted Hartree–Fock solution given that the molecular electronic configuration remains essentially single-reference. When a spin-contaminated solution arises, the energy splitting rapidly becomes large and $\langle \hat{S}^2 \rangle$ approaches the Hartree–Fock value; (ii) The VOO-CCD method, which is designed to approximate a multi-reference model, remains stable over broader ranges; however, for pure diradicals it becomes unstable. In these cases, spin-contamination is also very large, but the energy lowering for the spin-unrestricted solutions is negligible; (iii) Higher order corrections described by perturbation theory lead to smaller energy splittings between restricted and unrestricted (V)OO-CCD energies. However, in case of spin-contaminated (V)OO-CCD solutions, these corrections may lead to unphysical shapes of the potential energy surfaces. Thus, in order to quantitatively characterize the quality of the wave functions, both spin-contamination and energy lowering due to the breaking of spin-symmetry must be considered. © *2000 American Institute of Physics.* [S0021-9606(00)31439-8]

I. INTRODUCTION

Approximate solutions of the electronic Schrödinger equation do not always have the correct spacial symmetry and pure spin, i.e., are not eigenfunctions of the $\hat{S}^2$ and $\hat{S}_z$ operators. For example, Hartree–Fock equations[1,2] can have multiple solutions, of which the lowest energy one is not always a spin-pure function. Various types of such solutions have been classified by Fukutome,[3] and their nature and usefulness have been discussed by many researches.[4–11]

Correct spin-symmetry can be enforced by restricting the class of trial functions[3] at the cost of rising variational energy. Thus, one faces a choice (known as the symmetry dilemma[4]) between the best variational solution versus solution of the correct (spin) symmetry. The most general form of the Hartree–Fock ansatz is a Slater determinant composed of spin orbitals which may be admixtures of functions having α and β spins. The resulting Hartree–Fock wave function may have neither the correct projection of the total spin nor the correct magnitude of the total spin. This most unrestricted version of the Hartree–Fock model is called the General Hartree–Fock (GHF) method. If spin-orbitals are restricted to be functions of only α or β spins, but their spacial parts are allowed to be different, the resulting (spin) unrestricted Hartree–Fock (UHF)[12] wave function has a well-defined projection of the total spin, but may not be an eigenfunction of $\hat{S}^2$. In the restricted Hartree–Fock method (RHF) spin-orbitals are restricted to be functions of only α or β spins with the same spatial functions, and the Slater determinant is an eigenstate of both $\hat{S}_z$ and $\hat{S}^2$. The corresponding method for systems with unequal number of α and β electrons is called restricted open-shell Hartree–Fock (ROHF).

It has been recognized by earlier researchers that the existence of symmetry-broken or spin-contaminated solutions is not just a mathematical curiosity originating from the non-linear nature of the Hartree–Fock equations, but is rather an important source of information. The origin of these ''unphysical'' solutions is the breakdown of the mean-field model in cases where correlation effects become important for a qualitatively correct description, e.g., as in bond breaking. For example, in H_2 the appearance of the UHF solution at large nuclear separations signals that a single Slater determinant, $\Psi_{\mathrm{RHF}}=|\sigma(1)\alpha(1)\sigma(2)\beta(2)\rangle$, is no longer a good approximation of the molecular wave function. The UHF describes an electron localization near individual H atoms at the dissociation limit by using a single Slater determinant constructed from different α and β orbitals:

$$\Psi_{\mathrm{UHF}}=|s_1(1)\alpha(1)s_2(2)\beta(2)\rangle. \tag{1}$$

Though wave function Eq. (1) is only *half* of the correct solution (a mixture of triplet and singlet electronic configurations), and no longer has the correct space or spin symmetry, the UHF potential energy curve exhibits correct asymptotic behavior. Similar behavior can be found in other generic diradical[13] situations, such as in ozone or twisted

ethylene, or even in some predominantly closed shell molecules at equilibrium geometry, e.g., BH[8,9] and linear polyenes.

In all these examples, the existence of a spin-contaminated UHF solution, i.e., instabilities in the RHF method, is an indication for the importance of nondynamical correlation. Moreover, UHF is capable of describing certain physical effects omitted by RHF, e.g., electron localization at the dissociation limit. This enables the use of the UHF wave functions as an important source of information about correlation for more accurate methods, such as in a variety of projected and spin-constrained HF techniques,[14–21] through Pulay's unrestricted or half-projected HF based natural orbitals for multi-reference calculations,[22–24] or as a source of quadruple excitations in externally corrected coupled-cluster method of Paldus and co-workers[25] Sometimes UHF is considered as an alternative method for describing nondynamical correlation, though quantitatively the shape of the UHF potential energy curves and dissociation energies are far from being accurate,[26] and can even be completely wrong; e.g., the well known F_2 example.

Though correlated wave functions are more flexible than the single-determinant one, they can still be inappropriate for a particular system, e.g., single-reference models are qualitatively incorrect for bond-breaking processes. Thus it is instructive to analyze the spin-contaminated solutions in correlated wave functions in order to (i) gain better understanding of their limitations, and (ii) develop a diagnostic tool based on such unrestricted solutions. The purpose of this paper is to examine the spin-unrestricted solutions of coupled-cluster (CC) wave functions. This study is focused on singlet open-shell systems, where spin-contamination is attributed to nondynamical correlation. In systems with an uneven number of α and β electrons spin-contamination originates in the different mean-field experienced by α and β electrons (spin-polarization effect). It is unclear whether this effect can be attributed solely to nondynamical correlation. This question will be addressed in a future publication, where the results for high-spin open shell systems will be reported.

Since coupled-cluster singles and doubles model (CCSD)[27] is not variational, the discussion of spin-unrestricted CCSD solutions is somewhat ambiguous, because one cannot use the energy criterion when comparing spin-restricted and spin-unrestricted solutions of CCSD equations. On the other hand, CCSD is rather orbital-insensitive due to the presence of single excitations in the exponential ansatz, and one may expect that performing CCSD calculations with an unrestricted reference would reduce spin-contamination considerably. Stanton has investigated spin-contamination in the CCSD method for doublet radicals,[28] and has shown that it is indeed very small in both ROHF and UHF based CCSD calculations, even when the UHF spin-contamination is very large. For example, in NO_2 the value of $\langle \hat{S}^2 \rangle$ is 1.18 and 0.76 for UHF and UHF-based CCSD, respectively.[28] Similar behavior of the CCSD model has been reported for triplet states.[29,30] As far as singlet open-shell cases are concerned, the UHF-based CCSD energies have been found to be very different from the RHF-based values, e.g., the UHF-based CCSD (U-CCSD) potential energy curve[31] of F_2 shows the correct asymptotic behavior, in contrast to the RHF-based CCSD (R-CCSD). However, at intermediate separations U-CCSD energies are actually *higher* than R-CCSD and the U-CCSD curve exhibits an unphysical hump. Note that this spurious behavior of U-CCSD *cannot* be improved by the approximate spin-projection technique: Schlegel[32] has demonstrated that the CCSD energy with single annihilation, which removes the dominant contaminating component in the case of single bond breaking, is identical to the unprojected U-CCSD energy.[32]

Chen and Schlegel have investigated[33] spin-contamination for single bond breaking for a variety of UHF based single reference methods, e.g., Møller–Plesset theory of second (MP2) and fourth (MP4) orders, configuration interaction with double substitutions (CID), configuration interaction with single and double substitutions (CISD), quadratic CISD (QCISD), and coupled-cluster wave functions: CC doubles (CCD), CCSD, and projective Brueckner CCD (B-CCD) models. They have found[33] that at the dissociation limit the spin-contamination of all single reference methods approaches the Hartree–Fock value. However, the onsets for instabilities and spin-contamination in the intermediate region have been found to vary considerably for different methods. Not surprising, CC methods have demonstrated better stability and smaller spin-contamination than MPn and CI models. Moreover, the B-CCD model has demonstrated stability with respect to spin-symmetry breaking in a much wider range of nuclear distortions than CCSD. These findings[33] confirm that the propensity of the approximate wave function to break the spin-symmetry is directly related to the quality of employed approximations, and that spin-contamination can be viewed as an important diagnostic tool for judging the quality of approximate models.

Optimized orbitals coupled-cluster doubles (OO-CCD or OD) method[34,35,27] is the most appropriate model to address the question of the stability of restricted coupled-cluster wave functions with respect to the spin-symmetry breaking, since in this method the orbitals of the reference determinant are optimized to minimize the OO-CCD energy. The following questions are addressed: (i) How stable are coupled-cluster wave functions with respect to the spin-symmetry breaking? (ii) How large is the spin-contamination? (iii) How large is the energy lowering for spin-contaminated solutions? and (iv) How do the shapes of potential energy surfaces (PESs) change when higher order corrections[36,37] are applied to spin-symmetry broken solutions? The computationally demanding stability analysis[38,10] based on the orbital Hessians is not discussed here.

OO-CCD, as a single-reference method, is expected to exhibit triplet instability due to the unbalanced treatment of dynamical and nondynamical correlation.[39] Recently, we introduced a coupled-cluster model capable of describing nondynamical correlation effects, namely, the valence optimized orbitals coupled-cluster doubles (VOO-CCD or VOD).[39] The VOO-CCD method has been shown[39] to be a very accurate approximation of a full valence complete active space SCF (CASSCF)[40,41] model for single-bond dissociation and

diradicals. It is thus interesting to investigate the stability of the VOO-CCD model for triplet instability.

The paper is organized as follows: Sec. II briefly reviews the (V)OO-CCD model and discusses the calculation of $\langle \hat{S}^2 \rangle$, Sec. III presents several examples (bond-breaking in H_2, BH, F_2, HF; twisted ethylene, and ozone), and the conclusions are given in Sec. IV.

II. THEORY

In the (V)OO-CCD model,[27,35,34,39] the wave function has an exponential form, $e^{\hat{T}_2}\Phi_0$, where Φ_0 is a reference Slater determinant with orbitals optimized to minimize the total energy, and $\hat{T}_2$ is an operator of double excitations from the reference. The resulting equations for the amplitudes $\hat{T}_2$ and orbitals are:

$$\langle \Phi_0 | \hat{H} | (1+\hat{T}_2)\Phi_0 \rangle = E, \tag{2}$$

$$\langle \Phi_{ij}^{ab} | \hat{H} | (1+\hat{T}_2+\tfrac{1}{2}\hat{T}_2^2)\Phi_0 \rangle = E a_{ij}^{ab}, \tag{3}$$

$$\mathbf{C} = \mathbf{C}^o \mathbf{U}(\theta),$$

$$\frac{\partial E}{\partial \mathbf{U}(\theta)} \frac{\partial \mathbf{U}(\theta)}{\partial \theta} = 0, \tag{4}$$

where $\mathbf{C}$ is the molecular orbital matrix, $\mathbf{C}^o$ defines some set of guess orbitals, and $\mathbf{U}$ is the orbital transformation matrix defined by the set of orbital rotation angles θ. Equations (2) and (3) define the energy and $\hat{T}_2$ amplitudes in the CCD model, whereas Eq. (4) defines the variationally optimized orbitals. The final programmable equations for the energy, gradients with respect to orbital rotations and nuclear displacements, and an efficient method for solving Eqs. (2)–(4) are given in Ref. 34.

In OO-CCD model, where all the orbitals are active and the operator $\hat{T}_2$ is defined in a whole orbital space, only mixing between occupied and virtual orbitals must be taken into account. In the VOO-CCD model, only valence orbitals are made active, and the $\hat{T}_2$ operator now works only in the active orbital space. Thus, the VOO-CCD energy is optimized with respect to orbital rotations between four orbital subspaces (restricted occupied, active occupied, active virtual, and restricted virtual).[39]

Though both models are defined by the same set of equations, they aim to describe very different situations. OO-CCD is a strictly single-reference model and can be viewed as a size-extensive approximation of the full CI. It treats both dynamical and nondynamical correlation on similar footing, and is thus not capable of describing multi-reference situations. The VOO-CCD model is a size-consistent approximation to a full valence CASSCF wave function, and describes only nondynamical correlation. VOO-CCD[39] is thus an appropriate zero-order wave function for multi-reference situations. However, one has to include dynamical correlation corrections[36,37] in order to obtain accurate results. Dynamical correlation corrections for the VOO-CCD model are calculated by standard perturbation theory through second order, thus, we refer to the resulting method as VOO-CCD(2).[37] VOO-CCD(2) captures dynamical correlation effects through external single, double, and semi-internal triple and quadruple substitutions.[37] The initial benchmarks[37] have demonstrated that the VOO-CCD(2) method provides an inexpensive and robust way to describe diradicals and the breaking of single bonds with quantitative accuracy. In a similar fashion, effects of triple and quadruple excitations can be estimated for OO-CCD wave functions, i.e., by the OO-CCD(2) model.[36]

Operator $\hat{S}^2$ is a two-electron operator, and thus has the following form in second quantization:

$$\hat{S}^2 = \frac{1}{2} \sum_{pqrs} \langle pq|\hat{S}^2|rs\rangle p^+ q^+ sr, \tag{5}$$

where the sum is over all spin-orbitals, and $\langle pq|\hat{S}^2|rs\rangle$ are the matrix elements of the two-electron operator $\hat{S}^2(1,2)$:

$$\langle pq|\hat{S}^2|rs\rangle = \int d1\, d2\, \phi_p^*(1)\phi_q^*(2)\hat{S}^2\phi_r(1)\phi_s(2). \tag{6}$$

The expectation value of $\langle \hat{S}^2 \rangle$ is given by a contraction of $\langle pq|\hat{S}^2|rs\rangle$ with a corresponding reduced two-electron density matrix:

$$\langle \hat{S}^2 \rangle = \frac{1}{2} \sum_{pq} \langle pq|\hat{S}^2|rs\rangle \Gamma_{pqrs}. \tag{7}$$

For the coupled-cluster wave function, the density matrix can be found from response theory, or by considering the generalized ''CC expectation value'':

$$\Gamma_{pqrs} = \langle \Psi_L e^{-\hat{T}} | p^+ q^+ sr | e^{\hat{T}} \Psi_R \rangle, \tag{8}$$

where Ψ_L and Ψ_R are left and right eigenfunctions of the similarity transformed Hamiltonian, $\bar{H} = e^{-\hat{T}} H e^{-\hat{T}}$.

Further transformations of Eqs. (5)–(6) yield the following convenient expression for $\langle \hat{S}^2 \rangle$:[29,28]

$$\begin{aligned}\hat{S}^2 = \frac{1}{4}\Bigg[& (N_\alpha - N_\beta)^2 + 2(N_\alpha + N_\beta) \\ & + 2\sum_{pqrs} \Delta_{p\bar{r}}\Delta_{q\bar{s}}\Gamma_{p\bar{q}r\bar{s}} + 2\sum_{\underline{pqrs}} \Delta_{p\bar{r}}\Delta_{q\bar{s}}\Gamma_{p\bar{q}r\bar{s}}\Bigg] \\ = \frac{1}{4}(N_\alpha - N_\beta)^2 & + \frac{1}{2}(N_\alpha + N_\beta) + \sum_{pqrs} \Delta_{p\bar{r}}\Delta_{q\bar{s}}\Gamma_{p\bar{q}r\bar{s}},\end{aligned} \tag{9}$$

where N_α and N_β denote the number of α and β electrons, respectively, indexes p,q,r,s are used for α and indexes $\bar{p},\bar{q},\bar{r},\bar{s}$ for β spin-orbitals, and the matrix $\Delta_{p\bar{r}}$ is a spacial overlap between α and β spin-orbitals. The two-particle density matrix is defined by Eq. (8) and thus contains also the separable part. Explicit expressions for the two-particle density matrix for (V)OO-CCD wave functions can be found in Refs. 34, 42.

III. RESULTS AND DISCUSSION

We now consider two examples of chemically important situations when the accurate description of nondynamical correlation is essential, and where the instability of the RHF wave function is well known. We discuss (i) bond dissocia-

tion in diatomics (H_2, BH, F_2, and HF); (ii) diradical transition states (ethylene torsion); and (iii) the ozone molecule, which is known to have a significant diradical character.

In order to find unrestricted (V)OO-CCD solutions, we have used UHF molecular orbitals (or U-MP2 natural orbitals) as an orbital guess. In regions of stability, (V)OO-CCD models have been found to converge easily to a spin-pure solution.

All orbitals are active in OO-CCD calculations. The VOO-CCD calculations reported here are always performed in a full valence active space, with core orbitals restricted (except for the BH results where core orbitals are included in the active space).

The present study employs a double-ζ plus polarization (DZP) basis set of contracted Gaussian functions, comprised of the standard Huzinaga–Dunning[43,44] double-ζ basis augmented by six d-type polarization functions for first-row atoms [$\alpha_d(B)=0.5$, $\alpha_d(C)=0.75$, $\alpha_d(O)=0.85$] and three p-type polarization functions [$\alpha_p(H)=0.75$] for hydrogen. For BH, we used the p exponent for hydrogen [$\alpha_p(H)=1.0$] employed by Harrison and Handy.[45] The contraction scheme for the DZP basis is $(9s5p1d/4s2p1d)$ for first-row atoms and $(4s1p/2s1p)$ for hydrogen. For the F_2 molecule we use DZP+ basis set from Ref. 31, derived from the standard Huzinaga–Dunning[43,44] double-ζ (DZ) basis set by uncontracting the most diffuse p-function and augmenting it by a set of six Cartesian d-functions [$\alpha_d(F)=1.580$]. Calculations of HF are performed using split-valence 6-31G basis set.[46] To elucidate possible effects of dynamical correlation, some additional results are obtained with the STO-3G basis.[47]

Calculations are performed using two *ab initio* packages, Q-Chem[48] and PSI,[49] to which our program for (V)OO-CCD calculations is linked.

A. Single bond dissociation

The simplest example is H_2, where the UHF solution arises around 2.2 bohr, and the $\langle\hat{S}^2\rangle$ value rapidly approaches 1. This reflects the fact that the UHF solution Eq. (1) is a mixture of singlet and triplet configurations. As expected, OO-CCD, which is exact for two electrons, completely removes the spin-contamination and converges to the same energy as the spin-restricted version. Similarly, the VOO-CCD model, which is equivalent to the full valence CASSCF, also restores the spin-pure solution.

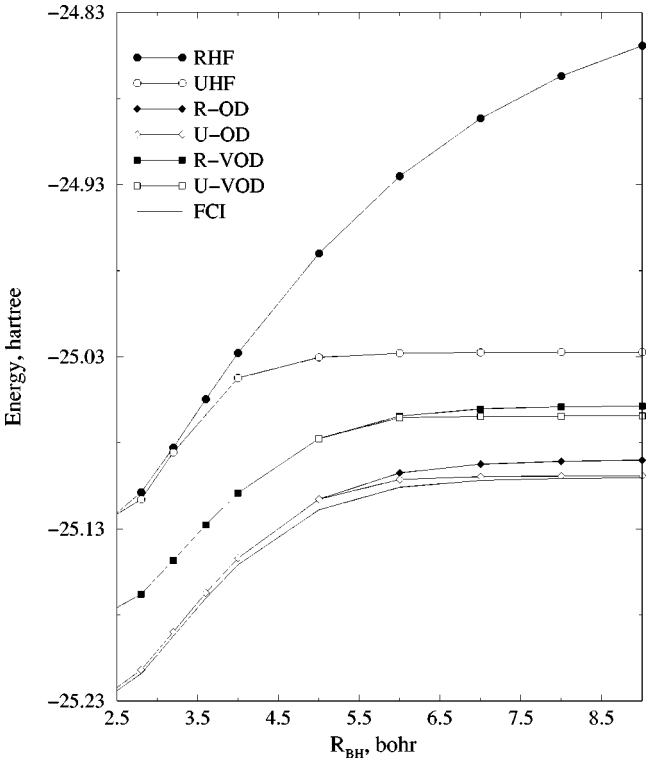

FIG. 1. Potential energy curves for BH, DZP basis set. The energy lowering due to spin-symmetry breaking is much smaller for the correlated OO-CCD model than for Hartree–Fock one. The VOO-CCD method, which is capable of describing multi-reference situations, remains stable over a broader range and exhibits much smaller energy lowering due to spin-contamination.

As a next example, consider BH. Restricted and unrestricted potential energy curves are shown in Fig. 1. Selected total energies and $\langle\hat{S}^2\rangle$ values are given in the Table I. BH has a ground electronic configuration $1\sigma^2 2\sigma^2 3\sigma^2$ and a large nondynamical correlation contribution originating in the $1\sigma^2 2\sigma^2 1\pi^2$ configuration. As a result, BH has UHF solutions even around the equilibrium geometry.[8,9] The UHF solution is about 0.2 eV lower than the RHF one, and gives

TABLE I. BH, DZP basis set. Total energies, hartree, and $\langle\hat{S}^2\rangle$ for Hartree–Fock and (V)OO-CCD[a] methods.

R_{BH}, bohr	E_{RHF}	E_{UHF}	$E_{R\text{-}OD}$	$E_{U\text{-}OD}$	$E_{R\text{-}VOD}$ (Ref. 39)	$E_{U\text{-}VOD}$	$\langle\hat{S}^2\rangle_{HF}$	$\langle\hat{S}^2\rangle_{OD}$	$\langle\hat{S}^2\rangle_{VOD}$
1.8	−25.075 615	−25.084 463	−25.175 537		−25.123 112		0.5384		
2.0	−25.109 534	−25.117 360	−25.209 390		−25.158 668		0.5125		
2.2	−25.123 260	−25.130 085	−25.223 427		−25.174 435		0.4844		
2.8	−25.108 813	−25.113 028	−25.212 126		−25.167 874		0.3943		
3.2	−25.082 794	−25.085 678	−25.189 993		−25.148 281		0.3343		
4.0	−25.027 868	−25.042 504	−25.147 136		−25.109 155		0.5767		
5.0	−24.969 968	−25.030 540	−25.112 751		−25.077 674		0.8956		
6.0	−24.925 296	−25.028 121	−25.097 660	−25.101 465	−25.064 497	−25.065 451	0.9764	0.6257	0.9749
7.0	−24.891 684	−25.027 568	−25.092 486	−25.099 749	−25.060 360	−25.064 744	0.9976	0.9010	0.9986
8.0	−24.866 939	−25.027 377	−25.090 785	−25.099 380	−25.059 160	−25.064 504	1.0032	0.9755	1.0050
9.0	−24.849 375	−25.027 281	−25.090 169	−25.099 247	−25.058 788	−25.064 394	1.0046	0.9941	1.0067
10.0	−24.837 316	−25.027 281	−25.089 920	−25.099 192	−25.058 664	−25.064 346	1.0050	0.9987	1.0071

[a]Only spin-contaminated lower energy solutions are shown.

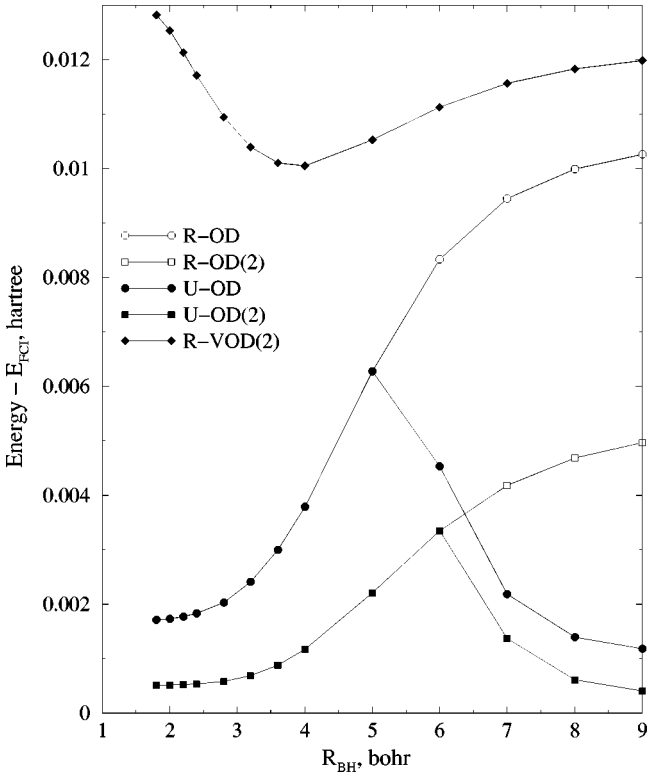

FIG. 2. Errors against FCI for restricted and unrestricted OO-CCD and OO-CCD(2), and restricted VOO-CCD(2) models. The relative errors for both R-OD(2) and U-OD(2) models, as well as energy splitting between spin-pure and spin-contaminated solutions, are considerably smaller than those of OD. However, the U-OD(2) still exhibits maximum relative error of 0.08 eV in the intermediate region, which is slightly larger than that of less expensive VOD(2) model.

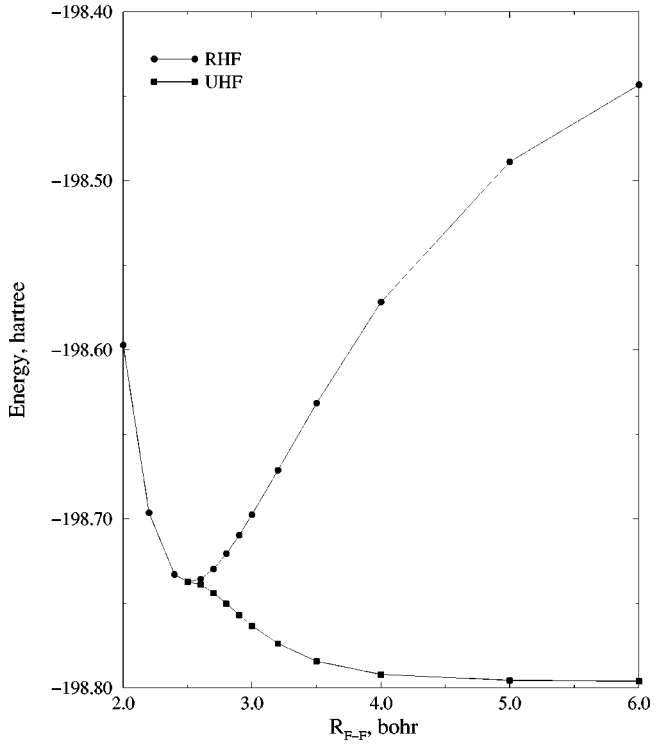

FIG. 3. RHF and UHF potential energy curves for F_2 molecule, DZP+ basis set. UHF fails to describe bonding in F_2.

$\langle \hat{S}^2 \rangle \approx 0.4$. As the B–H bond is stretched, $\langle \hat{S}^2 \rangle$ approaches unity and the energy difference between the RHF and the UHF solutions rapidly increases up to several eV.

OO-CCD restores the spin-pure solution at all nuclear separations up to 6 bohr, where a spin-contaminated lower energy solution arises. Though the spin-contamination of OO-CCD rapidly approaches unity, the energy lowering relative to the restricted solution does not exceed 0.25 eV. The dissociation energy obtained by unrestricted OO-CCD is very close to that of FCI[39] (error of 0.005 eV vs 0.25 eV for the restricted solution). However, similarly to the UHF method, the shape of the potential energy curve is not reproduced well, and there is a maximum relative error of about 0.14 eV in the intermediate region. The VOO-CCD spin-contaminated solution arises at approximately the same distance, but the energy lowering due to the spin-symmetry breaking is only 0.15 eV.

TABLE II. BH, DZP basis set. Total energies, hartree, for (V)OO-CCD(2)[a] method.

R_{BH}, bohr	R-OD(2)	R-VOD(2)	U-OD(2)
1.8	−25.176 732	−25.164 427	
2.0	−25.210 603	−25.198 591	
2.2	−25.224 674	−25.213 065	
2.4	−25.226 888	−25.215 708	
2.8	−25.213 581	−25.203 211	
3.2	−25.191 716	−25.182 005	
3.6	−25.169 398	−25.160 177	
4.0	−25.149 756	−25.140 876	
5.0	−25.116 819	−25.108 502	
6.0	−25.102 650	−25.094 866	−25.102 645
7.0	−25.097 749	−25.090 367	−25.100 559
8.0	−25.096 086	−25.088 942	−25.100 162
9.0	−25.095 463	−25.088 447	−25.100 025
10.0	−25.095 206	−25.088 257	−25.099 970

[a]Only spin-contaminated lower energy solutions are shown.

This example demonstrates that the correlated wave functions exhibit triplet instability at larger nuclear separation, and the energy lowering is much smaller than for the Hartree–Fock model, even though spin-contamination for both OO-CCD and VOO-CCD is almost the same as for UHF at large distances. Moreover, for VOO-CCD the energy difference between the restricted and the unrestricted solutions is very small, which is consistent with the accurate treatment of nondynamical correlation in this model.[39]

Using this example, we also investigate how the shapes of the PESs change when higher order corrections, (V)OO-CCD(2),[36,37] are applied to the spin-symmetry-broken solutions. Figure 2 shows errors against FCI for restricted and unrestricted OO-CCD, OO-CCD(2), and VOO-CCD(2). Based on these errors, we can see that inclusion of higher order corrections does not considerably change the shape of the unrestricted OO-CCD: the corrected curve still exhibits maximum relative errors in the intermediate region. However, the magnitude of the maximum relative error decreases from 0.14 eV for U-OD to 0.08 eV for U-OD(2). This error slightly exceeds the relative errors of the much less expensive restricted VOO-CCD(2) model. The important trend is that the energy splitting between spin-pure and

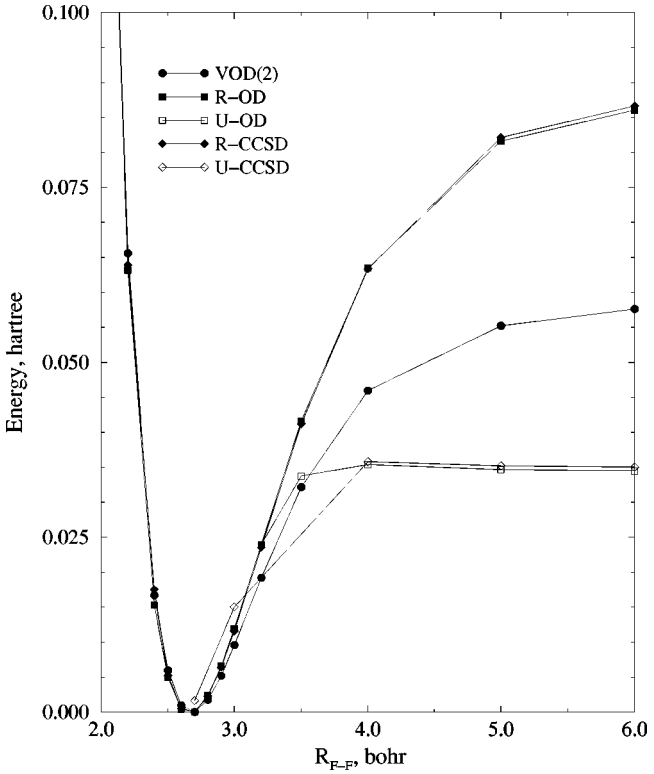

FIG. 4. Restricted and unrestricted potential energy curves for F_2 by the CCSD and OO-CCD methods, and by the VOO-CCD(2) model (DZP + basis set). All curves are shifted such that their respective energy minima are zero. The unrestricted OO-CCD curve is very close to R-CCSD at small distances and to the U-CCSD at the dissociation limit, and it does not have an unphysical hump. However, the dissociation energy is underestimated, as can be seen from comparison with the VOO-CCD(2) model.

spin-symmetry-broken solutions for OO-CCD(2) is considerably smaller than that for the OO-CCD model. Selected restricted (V)OO-CCD(2) energies are given in Table II. For this example, the VOD(2) procedure often becomes unstable when applied to the spin-symmetry broken VOD solution and yields complex-valued energy corrections. Similar behavior has been observed in F_2 for the unrestricted OD(2) model.

The next example is F_2. Its ground state configuration is $[\text{core}]3\sigma^2 4\sigma^2 1\pi^2 2\pi^2 3\pi^2 4\pi^2$, and there is only one valence unoccupied orbital, 5σ. Thus, here the VOO-CCD model is equivalent to the full valence CASSCF. F_2 is known (see, for example, Ref. 31) for being unbound at UHF level of theory (Fig. 3), and for its very strong dynamical correlation effects, e.g., full valence CASSCF underestimates the dissociation energy by a factor of 2.5.

The restricted and unrestricted CCSD[31] and OO-CCD, as well as VOO-CCD(2) curves, are shown in Fig. 4. Selected total energies and $\langle \hat{S}^2 \rangle$ values are given in Table III. Table IV presents equilibrium distances and dissociation energies for restricted and unrestricted CCSD, CASSCF, multi-reference CI and CC, and VOO-CCD(2) methods. Figure 4 demonstrates that the correlated U-CCSD wave function restores qualitatively the correct asymptotic shape of the potential, however, it exhibits an unphysical hump at intermediate distances. The spin-contaminated OO-CCD solution arises at 3.5 bohr, about the same distance where the U-CCSD energy becomes lower than the R-CCSD value. The unrestricted OO-CCD curve is smooth and close to the R-CCSD one where R-CCSD is lower in energy, and to the U-CCSD curve where it becomes lower in energy (this expected property of unrestricted OO-CCD originally motivated[50] the method development by Purvis and Bartlett[27]). The energy splitting between R-OD and U-OD is much larger than in the case of BH, because F_2 has more electrons and the imbalance in the treatment of nondynamical and dynamical correlation becomes more significant. Similarly to the U-CCSD curve and unlike the BH case, the dissociation energy is grossly underestimated.

VOO-CCD energies in this case are exactly the same as the full valence CASSCF energies.[31] No unrestricted VOO-CCD solutions has been found for F_2. Since the full valence CASSCF accounts fully for nondynamical correlation, this is not surprising, though it is unclear whether there is no spin-broken solutions for a full valence CASSCF in general.

Comparing the dissociation energies calculated by the different methods (Table IV), one can see that the U-CCSD value is only slightly better than R-CCSD one (the former overestimates D_e by 58%, and the latter underestimates it by 43%). The multi-reference CI and CC models used in Ref. 31 underestimate D_e by 16%. The VOD(2) model successfully recovers large contributions from dynamical correlation (full valence CASSCF underestimates D_e by 60%!), the resulting error of 9% being smaller than that of other multi-reference models.[31] Based on their results, Bartlett and coworkers have estimated[31] basis set limits for R_e and D_e to be 1.440 ± 0.0005 Å and 1.26 ± 0.05 eV, however, the excellent agreement of the VOO-CCD(2) values with experiment suggests larger value for the D_e's limit. Nevertheless, even if compared with the above limit for D_e, the U-CCSD value is still about 25% off (versus 87% for R-CCSD).

Another molecule for which the VOO-CCD model is equivalent to the full valence CASSCF calculation is HF. Its ground state configuration is $1\sigma^2 2\sigma^2 3\sigma^2 1\pi^2 2\pi^2$, and there is only one valence unoccupied orbital, 4σ. We consider this particular example in order to compare spin-contamination of OO-CCD with data for other single reference methods from Ref. 33. Figure 5 shows $\langle S^2 \rangle$ along the bond breaking coordinate for HF for the SCF, MP2, CISD, CCSD, B-CCD, and OO-CCD models. The values of $\langle S^2 \rangle$ shown in Fig. 5 are collected in Table V. As expected, MP2 theory does not significantly improve the spin-contaminated SCF wave function. The CISD model is more successful in reducing spin-contamination—the onset for CISD instability is further away, and spin-contamination is consistently smaller. The most interesting comparisons, however, are between (i) CISD and CCSD; (ii) CCSD and Brueckner CCD; and (iii) projective (B-CCD) and variational (OO-CCD) Brueckner CCD. CCSD reduces spin-contamination much better than CISD in the intermediate region, though onsets for instability are very close for both methods. The onset for the B-CCD model, however, is more than an angstrom further away than that of CCSD. Once reaching the instability region, the spin-contamination for B-CCD approaches that for CCSD very rapidly. The OO-CCD model has been found to become unstable at the same distance as B-CCD. Note, that except for

TABLE III. F_2, DZP+ basis set. Total energies, hartree, and $\langle \hat{S}^2 \rangle$ for Hartree–Fock, OO-CCD,[a] and VOO-CCD(2) methods.

R_{F-F}, bohr	E_{RHF} (Ref. 31)	E_{UHF} (Ref. 31)	$E_{R\text{-}OD}$	$E_{U\text{-}OD}$	$E_{R\text{-}VOD(2)}$	$\langle \hat{S}^2 \rangle_{HF}$	$\langle \hat{S}^2 \rangle_{OD}$
2.0	−198.597 306		−199.040 075		−199.029 086		
2.2	−198.696 599		−199.149 467		−199.140 076		
2.4	−198.733 109		−199.197 299		−199.188 930		
2.5	−198.737 428	−198.737 425	−199.207 648		−199.199 718	0.0004	
2.6	−198.735 725	−198.738 994	−199.212 176		−199.204 702	0.2182	
2.7	−198.729 734	−198.743 947	−199.212 593		−199.205 641	0.4189	
2.8	−198.720 781	−198.750 363	−199.210 205		−199.203 886	0.5624	
2.9	−198.709 852	−198.757 041	−199.205 994		−199.200 454	0.6669	
3.0	−198.697 670	−198.763 356	−199.200 678		−199.196 089	0.7441	
3.2	−198.671 451	−198.773 914	−199.188 632		−199.186 474	0.8461	
3.5	−198.631 568	−198.784 351	−199.170 972	−199.178 855	−199.173 475	0.9266	0.4515
4.0	−198.571 845	−198.792 184	−199.149 124	−199.177 214	−199.159 695	0.9797	0.8164
5.0	−198.488 966	−198.795 625	−199.131 010	−199.177 948	−199.150 446	1.0023	0.9810
6.0	−198.443 279	−198.796 141	−199.126 576	−199.178 114	−199.148 035	1.0047	0.9982

[a]Only spin-contaminated lower energy solutions are shown.

the onset point, where OO-CCD exhibits larger spin-contamination than B-CCD, the OO-CCD $\langle S^2 \rangle$ approaches the limiting value more slowly than the corresponding B-CCD value. Therefore, variational definition of the Brueckner orbitals allows to further improve the stability of the CCSD and B-CCD models. Energy lowering for U-OD relative to R-OD is similar to that in the previous examples.

B. Diradicals: Twisted ethylene and ozone

Even at the equilibrium geometry, the wave function of ethylene has significant contributions from the $(\pi^*)^2$ configuration. As the molecule is twisted and the double bond breaks, the $(\pi)^2$ and $(\pi^*)^2$ configurations soon become equally important. Figure 6 shows the potential energies calculated by the restricted and unrestricted methods. Total energies and $\langle \hat{S}^2 \rangle$ values are given in Tables VI, VII, and VIII. As in the previous example, the OO-CCD model remains stable in a fairly large range. It succeeds in restoring the spin-pure solution up to 60 degrees, even though the spin-contamination in UHF is very large. The unrestricted OO-CCD energy curve does not exhibit an unphysical cusp, and the energy difference between the restricted and unrestricted solutions is substantial at large angles. VOO-CCD spin-contaminated solution arises at 80 degrees. Though the spin-contamination of VOO-CCD is very large, the energy lowering due to spin-symmetry breaking is negligible, which agrees well with the very small deviation of VOO-CCD total energies from the full valence CASSCF even at 90°.[39] Moreover, unlike single-reference methods, the unrestricted VOO-CCD potential energy curve does not have a better shape than the restricted one: while the restricted VOO-CCD overestimates the barrier by 2.5 mhartree[39] relative to CASSCF, the unrestricted VOO-CCD underestimates it by 8.5 mhartree.

We have also performed calculations for the triplet state of ethylene at 90° (Table IX). With this basis set, the triplet state is found to be 4.2 mhartree below the singlet state for R-VOD and 7.9 mhartree above it for U-VOD.

Similar results have been obtained for ozone (Table X), however, spin-contamination of the OO-CCD and VOO-CCD wave functions is smaller than in the case of twisted ethylene, because in ozone a diradical configuration is not a leading one. The ground state electronic configuration of ozone is $[\text{core}]3a_1^2 2b_1^2 4a_1^2 5a_1^2 3b_1^2 1b_2^2 4b_1^2 6a_1^2 1a_2^2$, with a significant contribution from the $[\text{core}]3a_1^2 2b_1^2 4a_1^2 5a_1^2 3b_1^2 1b_2^2 4b_1^2 6a_1^2 2b_2^2$ configuration.

The observed instability of the VOO-CCD wave function may derive from:

(1) The absence of higher valence excitation in VOO-CCD, which is important for diradical species;
(2) Some (unexpected) indirect account of dynamical correlation through the orbital optimization procedure;
(3) The exponential form of the VOO-CCD wave function.

To find the correct answer, we have performed two-configurational SCF (TSCSF) calculations and minimal basis set calculations (Tables X,XI). Lower-energy spin-contaminated TCSCF solutions have been found in both twisted ethylene and ozone. In both cases energy lowering due to the singlet-triplet scrambling for the unrestricted

TABLE IV. Equilibrium distances and dissociation energies for F_2 molecule, DZP+ basis set.[a]

	R-CCSD (Ref. 31)	U-CCSD (Ref. 31)	CASSCF (Ref. 31)	MC-CISD (Ref. 31)	MC-LCCM (Ref. 31)	VOO-CCD(2)[b]	Expt.
R_e, Å	1.410	1.410	1.482	1.439	1.435	1.417	1.412
D_e, eV	2.36	0.95	0.67	1.22	1.22	1.51	1.66

[a]All multi-reference calculations (Ref. 31) have been obtained in the full valence active space.
[b]At R_e, VOO-CCD total energy is −198.812 457 hartree, and VOO-CCD(2) total energy is −199.205 707 hartree. D_e was computed as total energy difference at R_e and $R_{F-F}=100$ bohr.

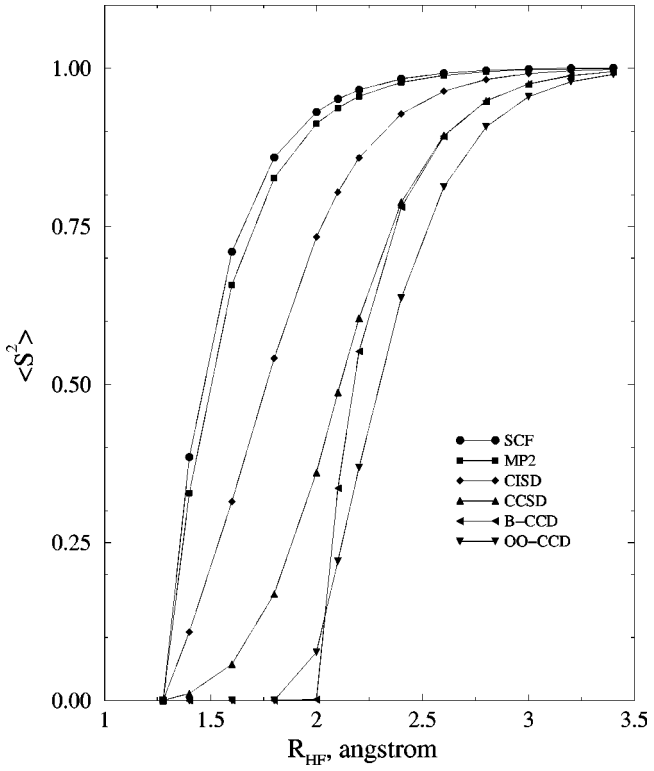

FIG. 5. $\langle S^2 \rangle$ along bond breaking coordinate for HF molecule, 6-31G basis set. On the dissociation limit, spin-contamination for all single-reference methods approaches the Hartree–Fock value. However, the onset of instability varies. The most stable methods with respect to spin-symmetry breaking are projective and variational Brueckner CCD, B-CCD and OO-CCD, respectively. Except for the onset point, where OO-CCD exhibits larger spin-contamination than B-CCD, the OO-CCD $\langle S^2 \rangle$ approaches limiting value slower than B-CCD, which rapidly merges with CCSD curve.

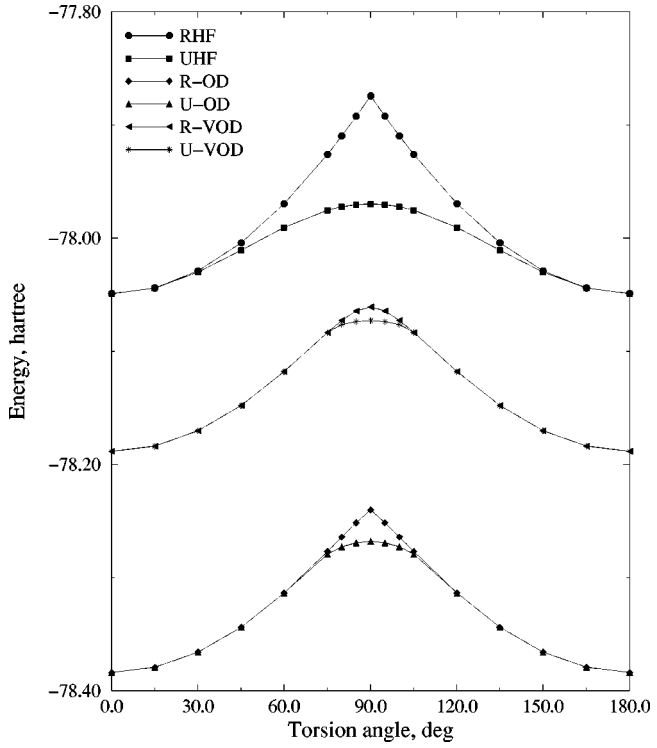

FIG. 6. Ethylene torsion, DZP basis. Unrestricted HF and OO-CCD potential energy curves do not exhibit unphysical cusp, however, the barrier height is underestimated. The energy lowering for spin-contaminated VOO-CCD solution is very small.

TCSCF is slightly larger than that for VOO-CCD. In ethylene, $\langle \hat{S}^2 \rangle$ for TCSCF is only slightly larger than $\langle \hat{S}^2 \rangle$ for VOO-CCD, however, in ozone the difference is more drastic—the TCSCF and VOO-CCD values of $\langle \hat{S}^2 \rangle$ are 0.93 and 0.26, respectively. Minimal basis set calculations (Table XI) demonstrated similar spin-contamination. Thus, we conclude that the existence of unrestricted solutions in the VOO-CCD model is a manifestation of the approximation made in nondynamical correlation calculations (absence of higher valence excitations). Very small energy lowering demonstrates that this approximation compromises the quality of VOO-CCD only slightly.

It is interesting to analyze why TCSCF and VOO-CCD behave similarly in twisted ethylene, and why the TCSCF spin-contamination and the energy lowering are much larger in ozone relative to VOO-CCD. We have analyzed the largest $\hat{T}_2$ amplitudes in both cases. In twisted ethylene, the largest value for $\hat{T}_2$ is 0.93 for the excitation from HOMO to LUMO ($\pi \rightarrow \pi^*$), and the magnitude of the next amplitude is 15 times smaller. That is why TCSCF provides a good description of the twisted ethylene. The situation in ozone is different. The largest VOO-CCD amplitude equals 0.25

TABLE V. HF, 6-31G basis set. $\langle \hat{S}^2 \rangle$ for Hartree–Fock, MP2, CISD, CCSD, B-CCD, and OO-CCD methods.

R_{F-F}, Å	HF (Ref. 33)	MP2 (Ref. 33)	CISD (Ref. 33)	CCSD (Ref. 33)	B-CCD (Ref. 33)	OO-CCD
1.4	0.3852	0.3282	0.1085	0.0112	0.0000	0.0000
1.6	0.7098	0.6575	0.3147	0.0573	0.0000	0.0000
1.8	0.8590	0.8264	0.5411	0.1687	0.0000	0.0000
2.0	0.9307	0.9122	0.7334	0.3607	0.0013	0.0764
2.1	0.9513	0.9376	0.8042	0.4872	0.3358	0.2207
2.2	0.9659	0.9557	0.8583	0.6045	0.5524	0.3686
2.4	0.9835	0.9778	0.9278	0.7880	0.7804	0.6368
2.6	0.9923	0.9890	0.9639	0.8938	0.8927	0.8126
2.8	0.9967	0.9947	0.9823	0.9481	0.9481	0.9075
3.0	0.9989	0.9975	0.9915	0.9751	0.9755	0.9554
3.2	1.0000	0.9989	0.9960	0.9883	0.9887	0.9790
3.4	1.0005	0.9996	0.9982	0.9947	0.9949	0.9905

TABLE VI. Ethylene torsion, DZP basis. Total energies, hartree, for CASSCF,[a] Hartree–Fock, OO-CCD,[a] and VOO-CCD[a] methods. Unoptimized barrier height, $\Delta E = E(90°) - E(0°)$, is also shown. Geometry used: $r_{CC} = 1.330$ Å, $r_{CH} = 1.076$ Å, $\alpha_{HCH} = 116.6°$.

Angle, deg.	CASSCF	RHF	UHF	R-OD	U-OD	R-VOD	U-VOD
0	−78.189 468	−78.049 241	−78.049 241	−78.383 854		−78.188 456	
15	−78.184 894	−78.044 220	−78.044 252	−78.379 377		−78.183 871	
30	−78.171 289	−78.029 202	−78.030 336	−78.365 974		−78.170 233	
45	−78.149 070	−78.004 332	−78.010 772	−78.343 854		−78.147 946	
60	−78.119 279	−77.969 898	−77.990 652	−78.313 661		−78.118 013	
75	−78.085 306	−77.926 371	−77.975 644	−78.277 105	−78.279 539	−78.083 581	
80	−78.075 076	−77.909 957	−77.972 601	−78.264 238	−78.272 976	−78.072 921	−78.076 398
85	−78.067 496	−77.892 646	−77.970 734	−78.251 669	−78.269 312	−78.064 617	−78.073 884
90	−78.064 613	−77.874 477	−77.970 105	−78.240 270	−78.268 139	−78.061 061	−78.073 065
ΔE, eV	3.40	4.76	2.15	3.91	3.15	3.74	3.14

[a]CASSCF, R-OD and R-VOD results are unreported data from previous study (Ref. 39).

$(1a_2 \rightarrow 2b_2$ excitation) and the next excitation $(1b_2 \rightarrow 2b_2)$ is only 3.5 times smaller. Since for these two excitations the occupied orbitals have different symmetries, it is clear that TCSCF is unable to describe the contribution of the second configuration. We expect this situation to be quite general: in many diradicals or bond-breaking processes lowering of the LUMO can cause large weights not only of a HOMO→LUMO excitation, but also for excitations from other valence orbitals.

We have also investigated how triple and quadruple excitations described perturbatively[36,37] affect the shapes of spin-restricted and spin-unrestricted curves. Figure 7 shows torsional potential for restricted and unrestricted VOO-CCD(2) and OO-CCD(2) models, and Table VII gives total energies for restricted and unrestricted (V)OO-CCD(2). As shown in Fig. 7, the shape of restricted OO-CCD(2) curve is considerably improved: it becomes more parallel to the VOO-CCD(2) one, and the amplitude of the unphysical sharp cusp of the restricted OO-CCD significantly decreases. Similarly to the BH example, the energy splitting between R-OD(2) and U-OD(2) is smaller than that between R-OD and U-OD. However, (2)-corrections do not improve the shape of the spin-symmetry broken OO-CCD: the U-OD and U-OD(2) curves are essentially parallel, and the VOD(2) frozen barrier height (Table VII) falls almost equally in between the R-OD(2) and U-OD(2) values. The effect of spin-contamination is even more dramatic for VOO-CCD, where the shape of the unrestricted VOO-CCD(2) curve is obviously unphysical. This result demonstrates that, unlike the spin-restricted case, it is difficult to improve the spin-symmetry broken model by a perturbative treatment of higher order effects.

IV. CONCLUSIONS

We have analyzed the spin-unrestricted solutions of the OO-CCD and VOO-CCD models for bond-breaking processes and diradical configurations. Since both methods are quasi-variational, the discussion of the stability of the corresponding wave functions is unambiguous and instructive. The main findings are:

(1) The OO-CCD method is stable for a relatively large range of nuclear distortions. It is capable of eliminating very large UHF spin-contamination (up to 0.8) given that the molecular electronic configuration remains essentially single-reference. When a spin-contaminated solution arises, the energy splitting rapidly becomes large and $\langle \hat{S}^2 \rangle$ approaches the UHF value. Similarly to UHF, the quality of the resulting potential energy surfaces is not satisfactory, e.g., the F_2 dissociation energy is grossly underestimated by the U-OD model.

(2) The VOO-CCD method, as an approximation of a multi-reference CASSCF model, remains stable over a broader range, however, for pure diradical situations (dissociation limit or twisted ethylene) it also becomes unstable. In these cases, the spin-contamination is very large and close to

TABLE VII. Ethylene torsion, DZP basis. Total energies, hartree, for OO-CCD(2) and VOO-CCD(2) methods. Unoptimized barrier height, $\Delta E = E(90°) - E(0°)$, is also shown.

Angle, deg.	R-OD(2)	U-OD(2)	R-VOD(2)	U-VOD(2)
0	−78.393 110		−78.360 532	
15	−78.388 706		−78.356 101	
30	−78.375 533		−78.342 879	
45	−78.353 855		−78.321 194	
60	−78.324 513		−78.292 011	
75	−78.289 979	−78.287 571	−78.258 441	
80	−78.278 495	−78.279 620	−78.247 933	−78.242 003
85	−78.268 143	−78.275 462	−78.239 344	−78.238 480
90	−78.260 502	−78.274 177	−78.234 468	−78.237 393
ΔE, eV	3.61	3.24	3.43	3.35

TABLE VIII. Ethylene torsion, DZP basis. $\langle \hat{S}^2 \rangle$ values for UHF, U-OD and U-VOD models.

Angle, deg.	UHF	U-OD	U-VOD
0	0.0003	0.0000	0.0000
15	0.0335	0.0000	0.0000
30	0.1934	0.0000	0.0000
45	0.4389	0.0000	0.0000
60	0.7186	0.0000	0.0000
75	0.9456	0.4773	0.0000
80	0.9935	0.7567	0.9530
85	1.0232	0.9145	1.0076
90	1.0333	0.9657	1.0229

TABLE IX. Energies, hartree, and $\langle \hat{S}^2 \rangle$ for the lowest triplet state of twisted ethylene, DZP basis.

Method	Energy	$\langle \hat{S}^2 \rangle$
HF	−77.965 445	2.0103
OO-CCD	−78.267 114	2.0004
VOO-CCD	−78.065 208	2.0067

TABLE X. Ozone, DZP basis. Total energies, hartree, and $\langle \hat{S}^2 \rangle$ for Hartree–Fock, TCSCF, OO-CCD, and VOO-CCD models. Geometry used: $r_e = 1.272$ Å, $\alpha = 116.8°$. Nuclear repulsion energy is 68.880 709 hartree.

Method	Restricted	Unrestricted	$\langle \hat{S}^2 \rangle$
HF	−224.312 197	−224.398 881	0.9328
TCSCF	−224.405 563	−224.409 496	0.9326
OO-CCD	−224.941 734	−224.943 408	0.2378
VOO-CCD	−224.534 184	−224.535 964	0.2626

TABLE XI. Energy lowering, mhartree, and $\langle \hat{S}^2 \rangle$ for twisted ethylene and ozone.

Method	Twisted C_2H_4	Ozone
HF/DZP	95.628 (1.0333)	86.684 (0.9328)
TCSCF/DZP	13.547 (1.0324)	3.933 (0.9326)
OO-CCD/DZP	27.869 (0.9657)	1.674 (0.2378)
VOO-CCD/DZP	12.004 (1.0229)	1.826 (0.2626)
HF/STO	205.324 (1.0417)	123.232 (0.9514)
OO-CCD/STO	186.073 (0.7240)	2.787 (0.2243)

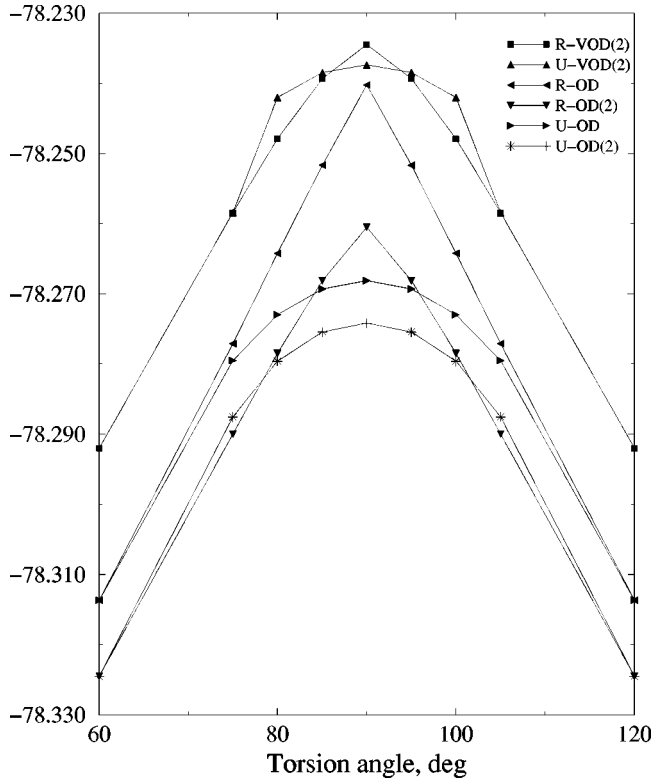

FIG. 7. Ethylene torsion, DZP basis. Higher order corrections when applied to spin-symmetry broken VOO-CCD solution result in unphysical shape of the potential curve. For restricted OO-CCD, perturbative treatment of triples and quadruples strongly decreases the amplitude of the cusp, and the corresponding OO-CCD(2) curve becomes closer to VOO-CCD(2) one. Unrestricted OO-CCD(2) curve is almost parallel to the unrestricted OO-CCD one, and thus also underestimate the barrier height.

the UHF one, but the energy lowering for the spin-unrestricted solutions is negligible.

(3) TCSCF demonstrates similar behavior, though in the case of ozone the TCSCF unrestricted solution has considerably larger spin-contamination than VOO-CCD. The reason for this effect is the absence of some valence double excitations with relatively large weights.

(4) Our analysis shows that the instability of the VOO-CCD model is due to the absence of higher valence excitations.

(5) Unlike the spin-restricted case, perturbative inclusion of triple and quadruple excitations does not always improve the shapes of PESs calculated by unrestricted models. However, the energy difference between the spin-pure and spin-contaminated solutions becomes smaller.

We conclude that the existence of spin-contaminated solutions reflects the quality of the employed wave function: if a model is qualitatively correct for a particular situation, it is expected to be stable. Therefore, analysis of the unrestricted solutions can be used as a diagnostic tool. In order to quantitatively characterize the quality of the wave functions, both the spin-contamination and the energy lowering due to the breaking of spin-symmetry must be considered, e.g., VOO-CCD exhibits very small energy lowering relative to OO-CCD, whereas the spin-contamination in both cases is large and close to the UHF one.

As far as the use of unrestricted solutions for the calcu-

lation of potential energy surfaces is concerned, our conclusion is negative. It is true that, for single-reference models, unrestricted curves represent definite advantages compared with the restricted ones, e.g., the cusp elimination in twisted ethylene, and (sometimes) improved dissociation energies. However, *quantitatively*, the improvement is not dramatic: for the F_2 example considered here the U-CCSD and R-CCSD errors are 43% and 42% (if compared with the experimental D_e), or 25% and 87% (if compared with multi-reference CI/CC). Moreover, it is unclear how one can systematically improve models employing spin-symmetry broken solutions: inclusion of higher order effects does not always improve the shapes of spin-contaminated PESs, i.e., in ethylene the most reliable estimation of the frozen barrier height [VOD(2) value] falls almost equally in between R-OD(2) and U-OD(2) values. No less important are the limitations imposed by working with a singlet-triplet scrambled wave function, the observed instability in (V)OD(2) procedure when applied to spin-symmetry broken reference, and sometimes the cumbersome procedure of breaking the spin-symmetry of the Hartree–Fock solution.[51] On the other hand, in cases where the wavefunction is essentially multi-reference, e.g., VOO-CCD or TCSCF, the energy lowering is anyway small and does not improve the PESs. Numerically, the performance of properly balanced models, i.e., when nondynamical correlation is included into zero-order wave function with a subsequent inclusion of dynamical correlation, is superior to that of unrestricted single-reference models.

ACKNOWLEDGMENTS

Acknowledgments are made to the Camille and Henry Dreyfus New Faculty Awards Program, to the James H. Zumberge Faculty Research and Innovation Fund at the University of Southern California, and to the Donors of the Petroleum Research Fund, administrated by the American Chemical Society for the support of this work. I wish to thank Dr. S. R. Gwaltney and Dr. C. D. Sherill for very stimulating and helpful discussions.

[1] D. R. Hartree, Proc. Cambridge Philos. Soc. **24**, 328 (1928).
[2] V. A. Fock, Z. Phys. **15**, 126 (1930).
[3] H. Fukutome, Int. J. Quantum Chem. **20**, 955 (1981).
[4] P.-O. Löwdin, Rev. Mod. Phys. **35**, 496 (1963).
[5] M. M. Mestechkin, *Rasshirennyi metod Khartri-Foka i ego primenenie k molekulam* (Kiev, Naukova Dumka, 1983).
[6] M. M. Mestechkin, *Nestabilnost' uravnenii Khartree-Foka i ustoichivost' molekul* (Kiev, Naukova Dumka, 1986).
[7] J.-L. Calais, Adv. Quantum Chem. **17**, 225 (1985).
[8] P.-O. Löwdin and I. Mayer, Adv. Quantum Chem. **24**, 79 (1992).
[9] P.-O. Löwdin and I. Mayer, Chem. Phys. Lett. **202**, 1 (1993).
[10] J. Paldus, ''Hartree–Fock stability and symmetry breaking,'' in *Self-Consistent Field: Theory and Applications*, edited by R. Carbó and M. Klobukowski, Vol. 70 (Elsevier, New York, 1990), pp. 1–45.
[11] D. B. Cook, ''The symmetry properties of the Hartree–Fock model: Some ''experimental'' results,'' in *Self-Consistent Field: Theory and Applications*, edited by R. Carbó and M. Klobukowski, Vol. 70 (Elsevier, New York, 1990), pp. 45–79.
[12] J. A. Pople and R. K. Nesbet, J. Chem. Phys. **22**, 571 (1954).
[13] L. Salem and C. Rowland, Angew. Chem. Int. Ed. Engl. **11**, 92 (1972).
[14] P.-O. Löwdin, Phys. Rev. B **97**, 1509 (1955).
[15] I. Mayer, Adv. Quantum Chem. **12**, 189 (1980).
[16] A. T. Amos and G. G. Hall, Phys. Rev. C **263**, 483 (1961).
[17] P.-O. Löwdin, ''The projected Hartree–Fock method: An extension of the independent particle model,'' in *Quantum Theory of Atoms, Molecules, and the Solid State* (Academic, New York, 1966), pp. 601–623.
[18] Y. G. Smeyers and L. Doreste-Suares, Int. J. Quantum Chem. **7**, 687 (1973).
[19] J. Baker, Chem. Phys. Lett. **152**, 227 (1988).
[20] J. S. Andrews, D. Jayatilaka, R. G. A. Bone, N. C. Handy, and R. D. Amos, Chem. Phys. Lett. **183**, 423 (1991).
[21] Y. G. Smeyers, ''Extended Hartree–Fock models: A comprehensive review,'' in *Self-Consistent Field: Theory and Applications*, edited by R. Carbó and M. Klobukowski, Vol. 70 (Elsevier, New York, 1990), pp. 80–135.
[22] R. G. A. Bone and P. Pulay, Int. J. Quantum Chem. **45**, 133 (1992).
[23] P. M. Kozlowski and P. Pulay, Theor. Chim. Acta **100**, 12 (1998).
[24] J. M. Bofill and P. Pulay, J. Chem. Phys. **90**, 3637 (1989).
[25] P. Piecuch, R. Tobola, and J. Paldus, Phys. Rev. A **54**, 1210 (1996).
[26] R. J. Bartlett and J. F. Stanton, Rev. Comput. Chem. **5**, 65 (1994).
[27] G. D. Purvis and R. J. Bartlett, J. Chem. Phys. **76**, 1910 (1982).
[28] J. F. Stanton, J. Chem. Phys. **101**, 371 (1994).
[29] G. D. Purvis III, H. Sekino, and R. J. Bartlett, Collect. Czech. Chem. Commun. **53**, 2203 (1988).
[30] D. H. Magers, R. J. Harrison, and R. J. Bartlett, J. Chem. Phys. **84**, 3284 (1986).
[31] W. D. Laidig, P. Saxe, and R. J. Bartlett, J. Chem. Phys. **86**, 887 (1987).
[32] H. B. Schlegel, J. Phys. Chem. **92**, 3075 (1988).
[33] W. Chen and H. B. Schlegel, J. Chem. Phys. **101**, 5957 (1994).
[34] C. D. Sherrill, A. I. Krylov, E. F. C. Byrd, and M. Head-Gordon, J. Chem. Phys. **109**, 4171 (1998).
[35] G. E. Scuseria and H. F. Schaefer, Chem. Phys. Lett. **142**, 354 (1987).
[36] S. R. Gwaltney and M. Head-Gordon, Chem. Phys. Lett. **323**, 21 (2000).
[37] S. R. Gwaltney, C. D. Sherrill, M. Head-Gordon, and A. I. Krylov, J. Chem. Phys. **113**, 3548 (2000).
[38] D. J. Thouless, *The Quantum Mechanics of Many-Body Systems* (Academic, New York, 1972).
[39] A. I. Krylov, C. D. Sherrill, E. F. C. Byrd, and M. Head-Gordon, J. Chem. Phys. **109**, 10669 (1998).
[40] B. O. Roos, P. R. Taylor, and P. E. M. Siegbahn, Chem. Phys. **48**, 157 (1980).
[41] K. Ruedenberg, M. W. Schmidt, M. M. Gilbert, and S. T. Elbert, Chem. Phys. **71**, 41 (1982).
[42] A. I. Krylov, C. D. Sherrill, and M. Head-Gordon, J. Chem. Phys. (to be published).
[43] S. Huzinaga, J. Chem. Phys. **42**, 1293 (1965).
[44] T. H. Dunning, J. Chem. Phys. **53**, 2823 (1970).
[45] R. J. Harrison and N. C. Handy, Chem. Phys. Lett. **95**, 386 (1983).
[46] W. J. Hehre, R. Ditchfield, and J. A. Pople, J. Chem. Phys. **56**, 2257 (1972).
[47] W. J. Hehre, R. F. Stewart, and J.A. Pople, J. Chem. Phys. **51**, 2657 (1969).
[48] J. Kong, C. A. White, A. I. Krylov, C. D. Sherrill, R. D. Adamson, T. R. Furlani, M. S. Lee, A. M. Lee, S. R. Gwaltney, T. R. Adams, H. Daschel, W. Zhang, P. P. Korambath, C. Ochsenfeld, A. T. B. Gilbert, G. S. Kedziora, D. R. Maurice, N. Nair, Y. Shao, N. A. Besley, P. Maslen, J. P. Dombroski, J. Baker, E. F. C. Bird, T. Van Voorhis, M. Oumi, S. Hirata, C.-P. Hsu, J. Baker, M. Challacombe, E. Schwegler, J. P. Dombroski, C. Ochsenfeld, N. Ishikawa, J. Florian, R. D. Adamson, A. Warshel, B. G. Johnson, P. M. W. Gill, M. Head-Gordon, J. A. Pople, Q-Chem 2.0: A high performance *ab initio* electronic structure program package, J. Comput. Chem. (in press).
[49] T. D. Crawford, C. D. Sherrill, E. F. Valeev, J. T. Fermann, M. L. Leininger, R. A. King, S. T. Brown, C. L. Janssen, E. T. Seidl, Y. Yamaguchi, W. D. Allen, Y. Xie, G. Vacek, T. P. Hamilton, C. B. Kellogg, R. B. Remington, and H. F. Schaefer III, PSI 3.0, PSITECH, Inc., Watkinsville, GA 30677 (1999).
[50] R. J. Bartlett (private communication).
[51] P. Pulay and R. Liu, J. Phys. Chem. **94**, 5548 (1990).